

Spin-charge coupling for dilute La-doped $\text{Ca}_3\text{Ru}_2\text{O}_7$

G. Cao,¹ K. Abboud,² S. McCall,¹ J. E. Crow,¹ and R. P. Guertin³

¹National High Magnetic Field Laboratory, Tallahassee, Florida 32310

²Department of Chemistry, University of Florida, Gainesville, Florida 32608

³Department of Physics and Astronomy, Tufts University, Medford, Massachusetts 02155

(Received 28 March 2000; revised manuscript received 24 April 2000)

$\text{Ca}_3\text{Ru}_2\text{O}_7$ is a Mott-like system with a narrow gap (≈ 0.1 eV). Very dilute doping of trivalent La ($\leq 5\%$) for divalent Ca prompts rapid and simultaneous changes in both the magnetic and transport properties, unambiguously illustrating the strong spin-charge coupling that characterizes $\text{Ca}_3\text{Ru}_2\text{O}_7$. The antiferromagnetic metallic phase unique to $\text{Ca}_3\text{Ru}_2\text{O}_7$ persists into $(\text{Ca}_{1-x}\text{La}_x)_3\text{Ru}_2\text{O}_7$ with $x=0.04$, which is followed by a fully metallic ground state with a quenching of the magnetic moment at $x=0.05$. A large sudden drop in the magnetoresistivity up to 20 T defines a transition that is highly hysteretic and becomes irreversible at low temperatures and with La doping. The impact of La doping on $\text{Ca}_3\text{Ru}_2\text{O}_7$ is much more drastic than that of Sr doping, implying the importance of the added electron from the La ion. Unlike Ca_2RuO_4 where ferromagnetism is instantly induced in the antiferromagnetic host by La doping, $\text{Ca}_3\text{Ru}_2\text{O}_7$ shows no ferromagnetic ordering when La doped, but readily becomes a ferromagnet in modest magnetic fields.

$\text{Ca}_3\text{Ru}_2\text{O}_7$ is a recently studied Mott-like system with a number of unique features.¹ It has a double Ru-O layered orthorhombic structure² and belongs to the Ruddlesden-Popper series, $\text{Ca}_{n+1}\text{Ru}_n\text{O}_{3n+1}$, with $n=2$. $\text{Ca}_3\text{Ru}_2\text{O}_7$ undergoes antiferromagnetic ordering at $T_N=56$ K and a metal-nonmetal transition at $T_M=48$ K with a unique antiferromagnetic metallic phase (AFM) intermediate between the paramagnetic metallic (PMM) and antiferromagnetic insulating (AFI) phases.¹⁻³ Distinguishing it from other Mott systems, $\text{Ca}_3\text{Ru}_2\text{O}_7$ undergoes very sharp and concomitant metamagnetic and negative magnetoresistive transitions at 6 T which lead to a field induced ferromagnetic metallic phase at $T < T_M$. The field-temperature phase diagram for $\text{Ca}_3\text{Ru}_2\text{O}_7$ (Ref. 1) displays a wealth of extraordinary physical properties characterized by abrupt temperature- or field-induced transitions that separate a variety of magnetic and electronic phases, which are highly anisotropic. $\text{Ca}_3\text{Ru}_2\text{O}_7$ can serve as an ideal model system to explore new physics unique to $4d$ electrons³ and address fundamental issues such as the complex interplay of spin and charge degrees of freedom characteristic of almost all strongly correlated systems.

The intra-atomic Coulomb interaction, U , for $\text{Ca}_3\text{Ru}_2\text{O}_7$ is believed to be comparable to the kinetic energy or bandwidth, W , characteristic of Mott-Hubbard systems. Results of recent optical and Raman studies indicate that $\text{Ca}_3\text{Ru}_2\text{O}_7$ is indeed delicately poised near a metal-nonmetal borderline⁴ with a charge gap of 0.1 eV for $T < T_M$.⁵ Thus any small perturbations may be expected to readily prompt drastic changes in the ground state.

In this paper, we demonstrate that the metal-nonmetal transition, the spin gap, the metamagnetic transition and saturation magnetic moment, and the high-field magnetoresistive transitions of $\text{Ca}_3\text{Ru}_2\text{O}_7$ are suppressed uniformly and rapidly by only slight substitution of the trivalent La for the divalent Ca. In addition, we present the detailed crystal structure of $\text{Ca}_3\text{Ru}_2\text{O}_7$ determined by single-crystal x-ray diffraction. The substitution of the larger trivalent La ion relaxes

the buckling of the Ru-O-Ru bond (ionic radius $r=1.03$ Å for La vs 1.00 Å for Ca), thus increasing W (bandwidth control), and adds an extra electron to the system (filling control). While the electrical resistivity is expectedly reduced as a result of La doping, the observations are very striking: (1) The impact of La doping is much stronger than that of Sr doping ($r=1.18$ Å),³ indicating a more critical role of the filling-control. (2) The AFM phase,⁶ persists surprisingly into a fully metallic ground state in $(\text{Ca}_{1-x}\text{La}_x)_3\text{Ru}_2\text{O}_7$ for $x=0.04$. (3) The magnetic moment, $1.7\mu_B/\text{Ru}$ (close to the expected $2.0\mu_B/\text{Ru}$ for the low spin state $^3T_{1g}$ of $4d^4$) is fully quenched for $x \leq 0.04$ whereas the critical field for the metamagnetic transition remains at 6 T. (4) A high-field transition in the resistivity is found, resulting in a total resistivity decrease of more than 85%. This transition shows an unusually large hysteresis and becomes even irreversible as La doping increases, mimicking that of $\text{Pr}_{1-x}\text{Ca}_x\text{MnO}_3$.⁷ (5) In sharp contrast to its sister compound Ca_2RuO_4 where La doping instantly induces antiferromagnetic to ferromagnetic ordering,⁸ $\text{Ca}_3\text{Ru}_2\text{O}_7$ shows no occurrence of ferromagnetism when La doped. However, it becomes strongly ferromagnetic in magnetic fields larger than 6 T through spin reorientation, demonstrating an unstable magnetic ground state typical of the layered ruthenates.

The magnetic-moment suppression accompanying the approach to the metallic ground state in $(\text{Ca}_{1-x}\text{La}_x)_3\text{Ru}_2\text{O}_7$ demonstrates persuasively that spin and charge are intimately associated and that the $4d$ electrons serve a dual function—to form the localized moment on the Ru site and to serve as carriers for the electrical conductivity. The preponderance of d -electron weight at the Fermi surface is supported by photoemission studies^{4,9} and local-density approximation calculations of the band structure of related ruthenates, where no evidence of s - or p -electron contribution to the density of states at the Fermi surface is found.¹⁰

Single crystals of $(\text{Ca}_{1-x}\text{La}_x)_3\text{Ru}_2\text{O}_7$ were grown in Pt crucibles using a flux technique described elsewhere.¹⁻³ The crystal structure of $\text{Ca}_3\text{Ru}_2\text{O}_7$ is determined by single-crystal

TABLE I. Atomic position in $\text{Ca}_3\text{Ru}_2\text{O}_7$.

Element	x	y	z
Ru	0.25192	0.86409	0.40135
Ca(1)	0.73703	0.30989	0.00000
Ca(2)	0.24336	0.41629	0.31139
O(1)	0.81582	0.34578	0.69846
O(2)	0.33745	0.88862	0.50000
O(3)	0.44737	0.06527	0.08109
O(4)	0.94891	0.16272	0.11546

x-ray diffraction using a Siemens $P3/pc$ x-ray diffractometer. X-ray diffraction was also performed on powdered single crystals of $(\text{Ca}_{1-x}\text{La}_x)_3\text{Ru}_2\text{O}_7$ ($x > 0$) using Siemens Θ - 2Θ powder diffractometers, and the metric refinement was carried out using 18–23 reflections. The La concentration was determined by energy dispersive x-ray (EDX). All results of x-ray diffraction and EDX indicated that the crystals studied were pure and without any second phase. Several different growth melts were performed for each composition to ascertain reproducibility, and the data shown are representative of these compositions. Resistivity was measured with a standard four-probe technique and magnetization with a Quantum Design superconducting quantum interference device (SQUID) magnetometer.

$\text{Ca}_3\text{Ru}_2\text{O}_7$ is an orthorhombic system with the $A2_1ma$ space group (or $Cmc2_1$ with a being the long axis). The tilting of the RuO_6 octahedra results in $a\sqrt{2}a' \times \sqrt{2}a' \times c$ lattice with $a = 5.3720(6)$ Å, $b = 5.5305(6)$ Å, and $c = 19.572(2)$ Å. The atomic positions are listed in Table I where (x, y, z) refer to the axes (a, b, c) , respectively.

Shown in Fig. 1 is the crystal structure of $\text{Ca}_3\text{Ru}_2\text{O}_7$ where views of the ac and ab planes provide a clear view of the layered nature and significant distortions. The distortions are particularly severe in the ac plane where the tilting of the RuO_6 octahedra is most pronounced. The differences in the degree of tilting among the octahedra along the a axis as compared to the b axis is responsible for the orthorhombic distortion. The tilting is clearly reflected in the Ru-O-Ru bond angles, which differ considerably from 180° . Within the planes, these angles alternate between 149.87° and 150.47° , while for Ru ions in adjacent layers the Ru-O-Ru angle is 152.13° , which is primarily within the ac planes. The orthorhombic distortions present in $\text{Ca}_3\text{Ru}_2\text{O}_7$ extend even to the individual RuO_6 octahedra, contorting them so that each of the six Ru-O bond lengths is slightly different, and O-Ru-O bond angles are bowed slightly away from 180° . Along the c axis, the Ru-O bond length for oxygen sandwiched between the two RuO_6 planes is 1.9910 Å, while the other Ru-O bond length is 1.9914 Å and this O-Ru-O bond angle is 177° . For each octahedron, the four Ru-O bonds that lie within the plane are all different, i.e., 1.9834 , 1.9872 , 1.9972 , and 2.0088 Å. The O-Ru-O bond angles are much closer to 180° within the plane, where they alternate between 179.42° and 179.53° .

Doping the larger La ion significantly reduces the orthorhombic distortion, and thus, the degree of the Ru-O-Ru buckling. This is clearly reflected in Fig. 2 where the a and b

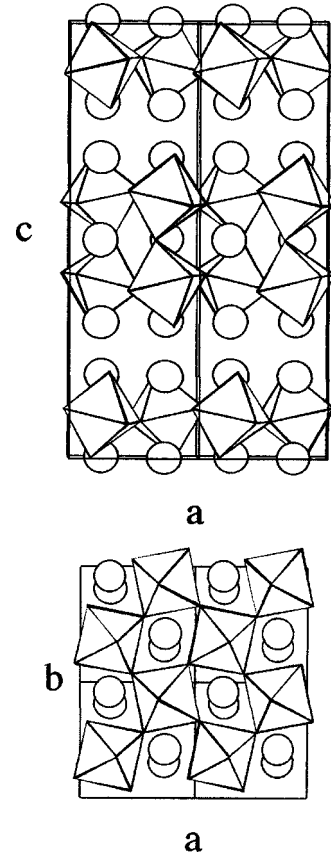


FIG. 1. The orthorhombic structure of $\text{Ca}_3\text{Ru}_2\text{O}_7$ showing the tilting and rotations of the RuO_6 octahedra in the ac plane (upper) and the ab plane (lower).

axis tend to merge as x increases. It is also noted that the c axis changes abruptly at $x = 0.03$.

Shown in Fig. 3(a) is the electrical resistivity, $\rho(T)$, for the a axis in the basal plane as a function of temperature for $(\text{Ca}_{1-x}\text{La}_x)_3\text{Ru}_2\text{O}_7$ with $x = 0, 0.01, 0.03, 0.04$, and 0.05 . (The a axis is the “easy axis” for magnetization to be discussed below, the c axis being perpendicular to the Ru-O planes.) Data for $x = 0.02$ are omitted for clarity. The sharp increase in $\rho(T)$ at $T_M = 48$ K becomes more rounded with increasing x , the onset of T_M decreasing with temperature and becoming fully suppressed for $0.03 < x < 0.04$. While the $x = 0.04$ sample is on the border of the metallic state with a close proximity to the insulating state, the $x = 0.05$ sample is

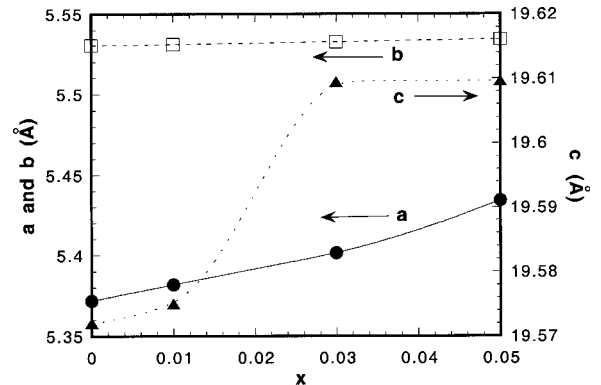


FIG. 2. The lattice parameters, a , b , and c , vs x .

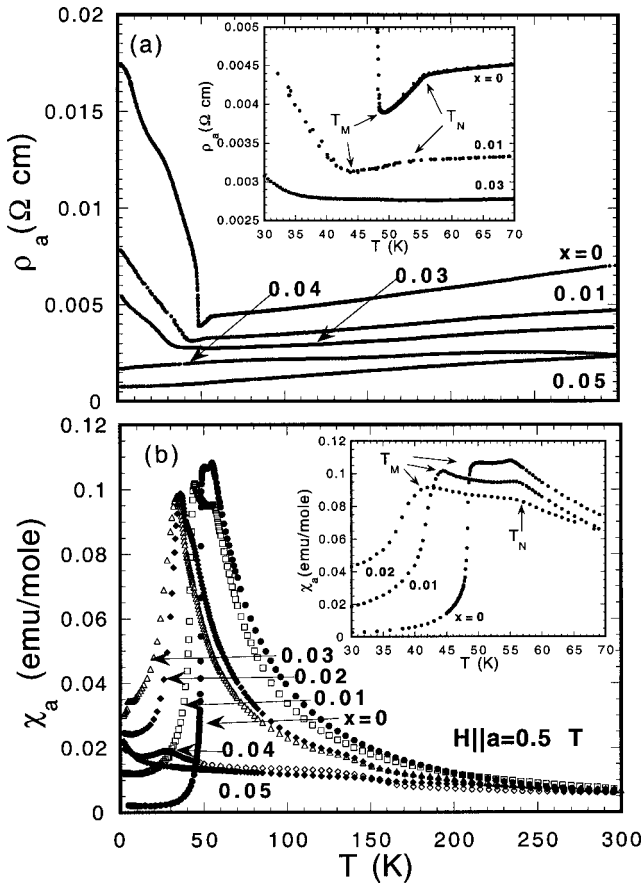


FIG. 3. (a) Electrical resistivity, $\rho(T)$, vs temperature for five $(\text{Ca}_{1-x}\text{La}_x)_3\text{Ru}_2\text{O}_7$ samples. Data for the $x=0.02$ sample are omitted for clarity. (b) Magnetic susceptibility vs temperature for six $(\text{Ca}_{1-x}\text{La}_x)_3\text{Ru}_2\text{O}_7$ samples with $H\parallel a$. Insets show details near the transitions.

fully metallic. For $50 < T < 250$ K, $\rho(T)$ is linear, suggesting non-Fermi-liquid type behavior, and for $T > 250$ K, $\rho(T) \approx \rho_0 + AT^2$ with coefficient $A \approx -8 \times 10^{-9} \mu\Omega \text{ cm/K}^2$. The inset of Fig. 1(a) shows details of the $\rho(T)$ anomalies at T_M and T_N , respectively, for $x=0, 0.01$, and 0.03 . The sharp decrease in $\rho(T)$ at T_N clearly indicates the onset of the antiferromagnetic metallic phase existing in a narrow yet well defined temperature range of $T_M < T < T_N$. This transition broadens as x increases.

The temperature dependence of the magnetic susceptibility, $\chi(T)$ defined as M/H , is shown in Fig. 3(b) for all six different concentrations from $x=0$ to 0.05 . The measuring field, H ($=0.5$ T), was along the easy axis. In all cases H was small enough that M vs H was linear so M/H represents the zero-field susceptibility, $\chi(T)$. Data were taken by field cooling, demonstrating unambiguously that the magnetic transitions, which are not hysteretic, are antiferromagnetic rather than ferromagnetic or canted antiferromagnetic transitions, which would yield some remanence on field cooling. The data above T_N shown in Fig. 3(b) were fit to a modified Curie-Weiss law, $\chi(T) = \chi_0 + C/(T - \Theta)$. For $150 < T < 350$ K the effective magnetic moment, p_{eff} , is $2.86\mu_B/\text{Ru}$ for $x=0$, nearly identical to that for the low-spin ($S=1$) value expected for the $\text{Ru}^{4+}(4d^4)$ ion ($2.83\mu_B/\text{Ru}$). The p_{eff} monotonically decreases to $2.71\mu_B/\text{Ru}$ for $x=0.01$, $2.52\mu_B/\text{Ru}$ for $x=0.02$ and $2.17\mu_B/\text{Ru}$ for $x=0.03$ but for

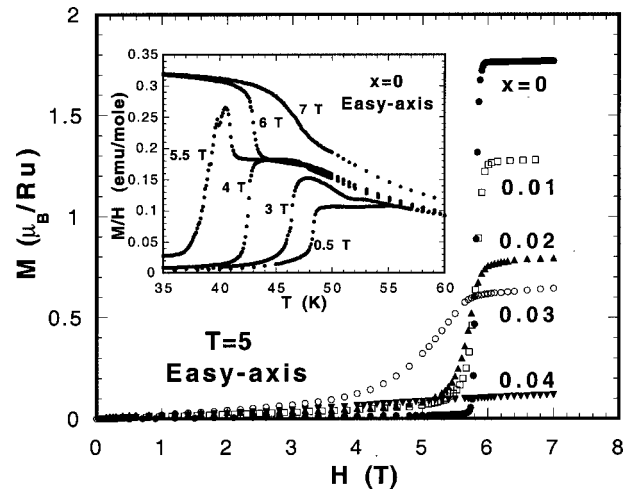


FIG. 4. Magnetization vs field at $T=5$ K for five $(\text{Ca}_{1-x}\text{La}_x)_3\text{Ru}_2\text{O}_7$ samples with $H\parallel a$. The transition field at 6 T is constant, even as the saturation magnetic moment is quenched with increasing x . The inset shows the magnetic susceptibility vs temperature at different fields for $\text{Ca}_3\text{Ru}_2\text{O}_7$. Note the sudden change at $H=6$ T.

$x=0.04$ and 0.05 , the fits to the modified Curie-Weiss law are unsatisfactory, implying possible spin fluctuations that are absent when the ground state is nonmetallic. The decrease in p_{eff} may be reflective of a slightly mixed valence Ru valence, driven by the trivalent La ion. It is noted that there is a weak anomaly around $T=150$ K for $x=0.04$. Whether this anomaly is intrinsic or due to a second phase is not yet clear. Nevertheless, this does not affect the conclusions drawn from these data.

The inset for Fig. 3(b) shows details of $\chi(T)$ for $x=0, 0.01$, and 0.02 at $T_N=56$ K and $T_M=48$ K, where the onset of the precipitous decrease in $\chi(T)$ may be used to define T_M . This anomaly is not characteristic of a typical antiferromagnet¹¹ and may be related to the opening of a spin gap in the electronic excitation spectrum due to a possible structural change. While there is no direct evidence for a structural transition occurring at $T_M=48$ K, a concomitant softening and broadening of an out-of-phase oxygen phonon mode for $T < T_M$ is observed in the Raman study,⁵ suggesting a strong modulation of d - p hybridization, or strong magnetoelastic coupling due to a strong modulation of the Ru-Ru interaction. Nevertheless, the abrupt drop at T_M followed by the nearly zero $\chi(T)$ at $T < T_M$ appears to be a nearly first-order transition leading to a ground state with a spin gap. Doping with La relaxes this constraint, and $\chi(T)$ approaches a finite value, as evident in $\chi(T)$, implying excitations above an increasingly smaller spin gap.

Shown in Fig. 4 is the magnetization $M(H)$, for the easy axis at $T=5$ K for $(\text{Ca}_{1-x}\text{La}_x)_3\text{Ru}_2\text{O}_7$ for all x showing the precipitous rise of $M(H)$ to saturation values, M_{sat} . All measurements were made after zero-field cooling the sample. With increasing La content, M_{sat} rapidly diminishes and is fully suppressed at $x=0.04$ even though the antiferromagnetism persists for this composition. This unambiguously associates the metamagnetic transition with the insulator to metal transition. It is surprising, however, that the critical

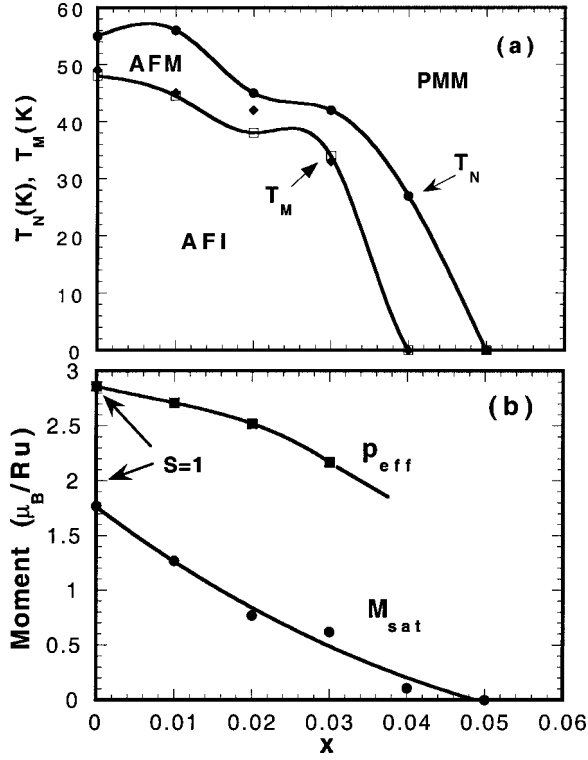


FIG. 5. (a) The Néel temperature, T_N , vs x and metal insulator transition temperature, T_M , for $(\text{Ca}_{1-x}\text{La}_x)_3\text{Ru}_2\text{O}_7$ delineating the three phases, PMM, AFM, and AFI. The T_M are determined both from the upturn in the electrical resistivity (filled diamonds) and from the peak in the magnetic susceptibility (open squares). The antiferro-magnetic metallic phase persists beyond the quenching of the AFI phase; (b) The saturated moment M_{sat} vs x , and effective moment, p_{eff} vs x .

field for the metamagnetic transition for $0 < x < 0.03$ remains sharply defined and essentially unchanged. The inset of Fig. 4 shows details of $M(H, T)$.

The La concentration dependence of the PMM, AFM, and AFI phases is illustrated in Fig. 5(a) which serves as a phase diagram. The metal-insulator transition is defined both from the temperature at which the resistivity $\rho(T)$ shifts from positive to negative temperature dependence and from the onset of the sudden decrease in $\chi(T)$. Both T_M and T_N decrease in a parallel fashion, and the AFM phase indeed exists almost in the entire doping range. For $x=0.05$, there is complete suppression of the AFI and AFM phases so the system remains fully metallic to the lowest measured temperature, albeit with high resistivity. The saturation moments, M_{sat} , are shown in Fig. 5(b) along with p_{eff} vs x . The $S=1$ values are indicated and close to those measured for $x=0$.

Figures 6(a) and 6(b) show the longitudinal magnetoresistivity in high fields along the easy axis for $x=0$ (a) and $x=0.03$ (b) for $T < T_M$. There are two distinct transitions, one at 6 T where the metamagnetic transition occurs, the other at higher fields which was not known before. The data exhibit a few noticeable features: (1) While the 6 T transition remains essentially unchanged as temperature and x vary, the high-field transition decreases quickly with increasing temperature and x . These two transitions are evidently driven by different mechanisms. The 6 T transitions are clearly associated with the metamagnetic transitions (Fig. 4). However, no corre-

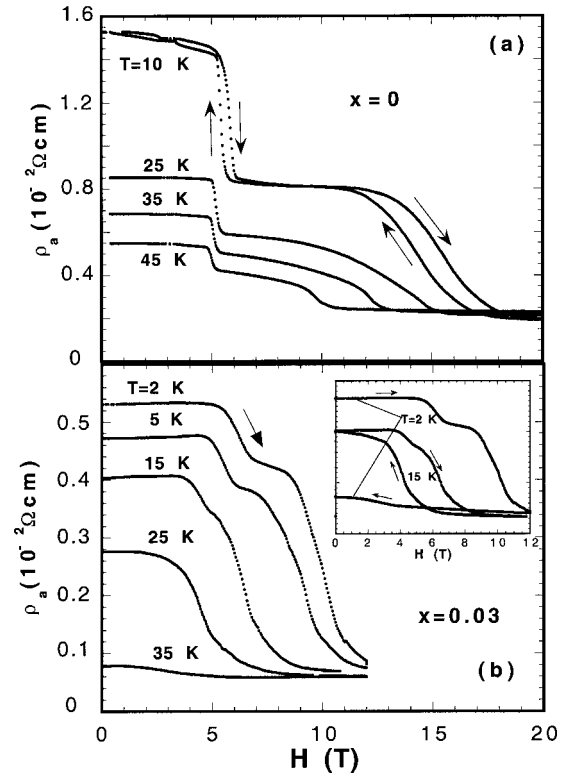


FIG. 6. (a) High-field isothermal magnetoresistance of $\text{Ca}_3\text{Ru}_2\text{O}_7$ for several temperatures. The low-field transition is simultaneous with the metamagnetic transition (see Fig. 2), the hysteretic upper-field transitions are new features, absent in the high-field magnetization. (b) Similar data for $x=0.03$. The inset shows details of the large hysteresis associated with the upper-field transitions.

sponding transition is seen up to 50 T in pulsed field $M(H)$ for the easy axis¹² (data not shown) on $\text{Ca}_3\text{Ru}_2\text{O}_7$. (2) The overall negative magnetoresistance ratio ($[\rho(0) - \rho(H)]/\rho(0)$), which is as high as 88%, is nearly identical for $x=0$ and 0.03 although the decrease at 6 T for $x=0.03$ becomes significantly smaller, which is consistent with the smaller metamagnetic rise in $M(H)$. (3) The higher-field transitions are so hysteretic that they become nearly irreversible at low temperatures for $x=0.03$ [inset of Fig. 6(b)]. This behavior is commonly seen in heavily doped manganites⁷ where the percolative effect is believed to be the origin. It is unclear whether this behavior seen in $(\text{Ca}_{1-x}\text{La}_x)_3\text{Ru}_2\text{O}_7$ can be attributed to the percolative effect, given such dilute La doping.

As mentioned above, a singular feature of $\text{Ca}_3\text{Ru}_2\text{O}_7$ is an observation in a stoichiometric compound at ambient pressure of the AFM phase¹ for $48 < T < 56$ K. Closely examining Fig. 2, we find it indisputable that the AFM phase persists up to $x=0.04$ where the AFM phase is characterized by the metallic behavior and well-defined antiferromagnetic ordering near $T_N=26$ K. This is supported by the data of Fig. 4: For $x=0.04$, the metamagnetic transition is completely absent, which unambiguously associates the 6 T metamagnetic transition with the AFI to AFM transition. For Mott systems where W is comparable to U , the AFM phase was predicted to be located either between the PMM and AFI phases as in $\text{Ca}_3\text{Ru}_2\text{O}_7$ or as a ground state alone as for

$0.04 < x < 0.05$. The calculation was based on a solution to the Mott-Hubbard Hamiltonian for the case of magnetic frustration involving the nearest- and the next-nearest neighbors.⁶ According to the model, the Néel temperature decreases as the degree of frustration increases and for intermediate frustration, the AFM phase arises. Because of this sensitivity, the AFM phase has never been seen in other stoichiometric materials at ambient pressure,¹³ so it is surprising that the AFM state in $\text{Ca}_3\text{Ru}_2\text{O}_7$ is insensitive to impurity doping.

One of the features of $\text{Ca}_3\text{Ru}_2\text{O}_7$, which was not fully addressed in our earlier paper,¹ is the abrupt first-order metamagnetic transition at $H=6$ T for $T < T_M$ that results in a nearly fully spin polarized metallic state with a saturated moment, M_{sat} , of $1.7\mu_B/\text{Ru}$ (vs expected $2\mu_B$ for $S=1$).¹ Our recent $\chi(T,H)$, as shown in the inset of Fig. 4, further confirms a field induced ferromagnetic (FM) state in $\text{Ca}_3\text{Ru}_2\text{O}_7$ that abruptly occurs at $H=6$ T. It needs to be emphasized that this spin-polarized metallic state is so spin-direction dependent that it exists only when H is parallel to the a axis. Otherwise $\text{Ca}_3\text{Ru}_2\text{O}_7$ remains nonmetallic below T_M with a low magnetic moment until $H \gg 6$ T.¹⁴ This intriguing behavior seemingly suggests an astonishing similarity to that of a half-metallic ferromagnet in which one spin channel is metallic while the other spin channel is insulating.¹⁵ More importantly, the precipitous transition from the AFM to the FM state resolutely indicates a highly unstable ground state due to a strong competition between AFM and FM coupling commonly seen in almost all layered ruthenates.^{3,8,16-18}

The metamagnetism in a Mott-Hubbard system was theoretically predicted using a single-band model.¹⁹ Based on this model, the metamagnetic transition is a function of the effective mass which is highly spin dependent. A discontinuous change in the effective-mass enhancement factor in magnetic fields is then expected to lead to a first-order metamagnetic transition to a magnetically saturated state. In this state where all electrons are presumably in the majority spin subband, the system is expected to be fully localized.¹⁹ In $\text{Ca}_3\text{Ru}_2\text{O}_7$, the metamagnetic transition characterized by the discontinuous jump in $M(H)$ may indeed be first order,²⁰ however, the magnetically saturated state antithetically becomes much more *metallic* (as seen in Ref. 1 and Fig. 6 above). This discrepancy, which could be due to a possible existence of multiple bands in $\text{Ca}_3\text{Ru}_2\text{O}_7$ where the single-band model can no longer be applicable, is striking and certainly merits thorough studies. Nevertheless, it is likely that the field-induced transition may precipitate a sudden change

at the Fermi surface that leads to a rapid disappearance of the narrow gap (0.1 eV) and/or a strongly ferromagnetic state that favors a metallic ground state.

The results presented in this paper are in sharp contrast with those of other related systems. In the case of $(\text{Ca}_{1-x}\text{Sr}_x)_3\text{Ru}_2\text{O}_7$, all distinctive magnetic and transport properties of $\text{Ca}_3\text{Ru}_2\text{O}_7$ are nearly retained for about $x=0.30$.³ The much more drastic changes seen in $(\text{Ca}_{1-x}\text{La}_x)_3\text{Ru}_2\text{O}_7$ suggest a remarkably critical role of the added electron from the La ion. Similarly, the suppression of the insulating phase is attained much more readily in the single layered $(\text{Ca}_{1-x}\text{La}_x)_2\text{RuO}_4$ (Ref. 8) than in $(\text{Ca}_{1-x}\text{Sr}_x)_2\text{RuO}_4$.²¹ It is also interesting to note that in spite of the similar monotonic depression of T_M in $(\text{Ca}_{1-x}\text{La}_x)_2\text{RuO}_4$ (Ref. 8) and $(\text{Ca}_{1-x}\text{La}_x)_3\text{Ru}_2\text{O}_7$, the magnetic properties are quite dissimilar. Even though both systems for $x=0$ have antiferromagnetic insulating ground states, La doping in $(\text{Ca}_{1-x}\text{La}_x)_2\text{RuO}_4$ even for concentrations as low as $x=0.005$, causes hysteretic ferromagnetic behavior. However, for $(\text{Ca}_{1-x}\text{La}_x)_3\text{Ru}_2\text{O}_7$ antiferromagnetic order is preserved even up to $x=0.05$ at which the magnetic moment is fully quenched. It is apparent that the double layered series is less sensitive than its single layer counterpart to a crossover from antiferro- to ferromagnetic ordering *by changing composition*, however, it is much more easily tipped to a strongly ferromagnetic ground state *by applying modest magnetic fields*. These distinct differences point to the very same feature that characterizes the layered ruthenates: a highly unstable ground state due to a strong competition between FM and AFM coupling.^{2,3,7,17,18,21} This point is also supported by recent theoretical studies indicating that ferromagnetic and antiferromagnetic fluctuations do coexist in the Ruddlesden-Popper Ca- and Sr-based ruthenates.¹⁶

The work presented in this paper underscores the extreme sensitivity of the Ca-based ruthenates to band filling effects and the intimate connection between the magnetic properties characterized by the magnetic moment and magnetic ordering and the proximity of the resistivity anomaly associated with a metal-nonmetal transition. In addition the work underlines the dual functions of d electrons at the Fermi surface which determine both magnetic moment formation and electronic carrier transport.

We would like to thank V. Dobrosavljevic for useful discussions. The work carried out at NHMFL was supported by the National Science Foundation under Cooperative Agreement No. DMR95-27035, NHMFL In-House Research Program grant and the State of Florida. R.P.G. was supported in part by the Research Corporation.

¹G. Cao, S. McCall, J. E. Crow, and R. P. Guertin, Phys. Rev. Lett. **78**, 1751 (1997).

²For review, G. Cao, C. S. Alexander, S. McCall, J. E. Crow, and R. P. Guertin, Mater. Sci. Eng., B **63**, 76 (1999).

³G. Cao, S. C. McCall, J. E. Crow, and R. P. Guertin, Phys. Rev. B **56**, 5387 (1997).

⁴A. V. Puchkov, M. C. Schabel, D. N. Basov, T. Startseva, G. Cao, T. Timusk, and Z.-X. Shen, Phys. Rev. Lett. **81**, 2747 (1998).

⁵H. L. Liu, S. Yoon, S. L. Cooper, G. Cao, and J. E. Crow, Phys.

Rev. B **60**, R6980 (1999).

⁶See, for example, G. Kotliar and G. Moeller, *Spectroscopy of Mott Insulators and Correlated Metals*, edited by A. Fujimori and Y. Tokura (Springer, Berlin, 1995), pp. 15-27.

⁷Y. Tomioka, A. Asamitsu, H. Kuwahara, Y. Moritomo, and Y. Tokura, Phys. Rev. B **53**, R1689 (1996).

⁸G. Cao, S. McCall, V. Dobrosavljevic, C. S. Alexander, J. E. Crow, and R. P. Guertin, Phys. Rev. B **61**, R5053 (2000).

⁹A. V. Puchkov, Z.-X. Shen, and G. Cao, Phys. Rev. B **58**, 6671

- (1998).
- ¹⁰I. I. Mazin and D. J. Singh, Phys. Rev. B **56**, 2556 (1997).
- ¹¹S. Foner, J. Appl. Phys. **39**, 411 (1968).
- ¹²Pulsed field measurements performed at National High Magnetic Field Laboratory, Los Alamos National Laboratory.
- ¹³In the phase diagrams of $\text{NiS}_{1-x}\text{Se}_x$ and V_2O_3 there is a narrow range of the AFM phase that is driven by varying pressure or composition. See, for example, F. Gautier, G. Krill, M. F. Lapi-erre, P. Panissod, C. Robert, G. Czjzek, J. Fink, and H. Schmidt, Phys. Lett. **53A**, 31 (1975); S. A. Carter, T. F. Rosenbaum, P. Metcalf, J. M. Honig, and J. Spalek, Phys. Rev. B **48**, 16 841 (1993).
- ¹⁴G. Cao (unpublished).
- ¹⁵See, for example, W. E. Pickett, Phys. Rev. Lett. **77**, 3185 (1996).
- ¹⁶I. I. Mazin and D. J. Singh, Phys. Rev. Lett. **82**, 4324 (1999).
- ¹⁷G. Cao, S. C. McCall, M. Shepherd, J. E. Crow, and R. P. Guertin, Phys. Rev. B **56**, 321 (1997).
- ¹⁸G. Cao, S. C. McCall, J. Bolivar, M. Shepherd, F. Freibert, P. Henning, and J. E. Crow, Phys. Rev. B **54**, 15 144 (1996).
- ¹⁹J. Spalek and W. Wojcik, in *Spectroscopy of Mott Insulators and Correlated Metals* (Ref. 6), pp. 41–65.
- ²⁰S. McCall, Ph.D. thesis, Florida State University, 2000. The as-
sertion of the field-induced first-order transition is also sup-
ported by an unusually large latent heat observed in measure-
ments of specific heat at $H=6$ T which is absent at $H=6$ T.
- ²¹G. Cao, S. McCall, M. Shepherd, J. E. Crow, and R. P. Guertin, Phys. Rev. B **56**, R2916 (1997).